[SSC19-WP1-08]

# Mission Dodona: Electronic Power System Design, Analysis and Integration

Sriram Narayanan, Rahul Rughani, Rebecca Rogers, Kyle Clarke, Jeremy Allam
University of Southern California, Information Sciences Institute and Space Engineering Research Center
4676 Admiralty Way, Suite 1001, Marina del Rey, CA 90292; (310)-448-8444
sriramn@usc.edu

## ABSTRACT

"Dodona" is USC's third CubeSat mission, and the electronic power system for this mission conforms to a centralized architecture common to the early-CubeSat class. The electronic power system is designed to power all satellite system components and any additional customer payload. A power budget is presented describing various operating configurations of the CubeSat and how its requirements are met in the design. The power system used a legacy Clyde Space 3U CubeSat Power System consisting of a combination of batteries and an Electronic Power System (EPS) to control charging, discharging, and voltage conversions for the system. The central architecture uses three major power lines to distribute power across the satellite, each subject to further regulation based on subsystem requirements. The system is reasonably efficient and has a high degree of utility, with significant heritage. This research discusses this centralized power system design and the testing methodology we used to validate, uncover and rectify issues prior to launch. While integrating the power system with other components on the satellite, problems were discovered and resolved through extensive testing. This paper presents insight into the operation of a nanosat electronic power system and the validation required to prepare it for flight.

## INTRODUCTION

Simulation and analysis is an important part of the power system design process, but often overlooked is the importance of rigorous integration and testing procedures. The highest quality simulation can never replicate the real world entirely, so integration and testing is as crucial of a mission component as design and simulation. On the DODONA mission, integration and testing played a key role in validating the design used and identifying issues that could not be found through simulation and analysis.

## DESCRIPTION OF THE POWER SYSTEM

Due to mission requirements, the electrical power system (EPS) is expected to support operations of the spacecraft including all additional payloads during periods in and out of eclipse. The choice of orbit and mission specifications will be detailed in the analysis section of the paper. The power system selected is an off the shelf component obtained from Clyde Space Ltd. Figure 1 depicts the architecture of the power system in a simplified manner.

### *Deployable Power System Module*

The power system works on the principle of Maximum Power Point Tracking of the solar arrays. A logic circuit is responsible for maintaining maximum input from the solar arrays during periods of high demand by simply tracking the voltage between a pair of panels connected to the same battery charge regulator (BCR) and drawing power from the one at a higher voltage level. The system is robust enough to drift array voltage from maximum voltage to open circuit levels when the satellite power demands are not high.

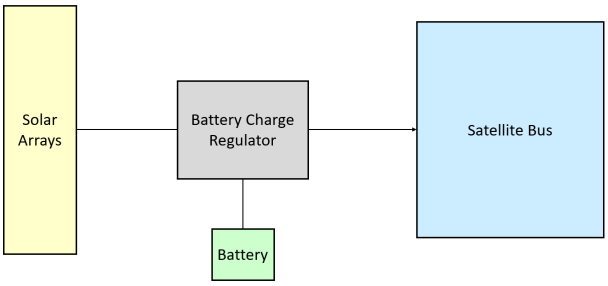


**Figure 1: Simplified Power System Layout**

In this architecture, the BCR is a buck DC-DC converter controlled in two modes of operation: maximum power point mode and end of charge mode. The system operates in the first mode during the charging phase of the battery, on complete recharge the BCR moves into its second mode. It uses a taper charge method to switch between the two modes. At end of charge the BCR regulates its output by allowing the input voltage from the arrays to drift away from maximum power levels.

There is a total of five BCRs available on the Clyde space deployable power system module of which DODONA will be using four to draw input from a total of seven

panels. Each one of these four BCRs is rated to a maximum of 8W. The output of all BCRs are connected and they supply charge to the battery and the power conditioning modules. The conditioning modules then distribute power across the satellite using three different power lines along the PC-104 interface. The following table shows maximum ratings for each one of these lines.

**Table 1: Power Line Specifications**

| Power Line | Voltage | Current Limit |
|---|---|---|
| VBATT | 7.8 V | 4.2 A |
| 5 V Line | 5 V | 1.2 A |
| 3.3 V Line | 3.3 V | 1 A |

The 5 V and 3.3 V regulators operate at a full load of approximately 90%. Further, the three main lines are protected using dedicated over-current protection switches. When an overcurrent is detected the switches open and prevent damage to the satellite bus. The system then periodically checks to see if the issue has cleared and turns on when ideal conditions have been restored.
The module also allows telemetry and telecommand through an $I^2C$ digital interface. Individual telecommands are available to reset the three voltage buses and telemetries such as array voltage, temperature and current; battery voltage and current; and each bus current can be queried. As per manufacturer specifications, the power consumption of the entire system is below 0.4 W.

***Battery System***

DODONA uses a 30 W h battery system from Clyde Space Ltd. The system comprises of a 20 W h board and an additional 10 W h module to extend capacity without any loss in protection. The battery is isolated from the electronic power system via two switches. The remove before flight (RBF) switch isolates the battery from the BCR input and the separation switch isolates the 3.3 V and 5 V regulators from the battery power. Figure 2 depicts the working of these switches.
The battery system uses lithium polymer cells with a rated capacity of 1320 mA h and a nominal voltage of 3.7 V. The main battery board (DBB) is divided into two layers, the lower level and the upper level each of which house two cells in series. However,the two levels themselves are connected in parallel. This board is connected to the rest of the spacecraft via the PC-104 interface. An additional 10 W h remote battery board is housed in the Bus In/ Bus Out board which is a passive user board to provide the payload area of the satellite with the full 104-pin bus. The $I^2C$ node on the remote battery board (RBB) is accessed via a 20-way JAE connector on this user board, four standoffs connect to the battery terminals. This board acts only as an extension, charging and discharging happens as normal.

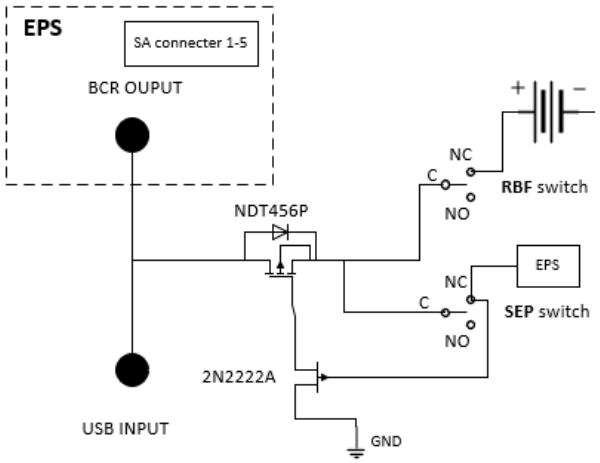


**Figure 2: Power System Switch Configuration**

Additionally, each battery board is provided with a thermostatically controlled heater which turns on automatically should the battery temperatures fall below 0 °C, they turn off when the temperature rises above 5 °C. Each battery board has a maximum charge voltage of 8.2 V and a minimum discharge voltage of 6.4 V. Both battery boards are built with over current protection using fuses. Over voltage and under voltage protection is extended when the battery system is integrated with the electronic power system (EPS).

***Solar Panel Specification***

DODONA uses a total of seven solar panels obtained from Pumpkin Space Systems, of which four are deployable and three are body mounted. Each one of these panels comprise six UTJ-class solar cells from Spectrolab. Nominal power output from a single panel is 6 W.As mentioned previously, the panels are connected to the electronic power system based on the maximum power point tracking principle, each used BCR is paired with two solar panels and only one can be lit at a given time as the BCR is rated to a maximum of 8 W. Due to this constraint, and the mission design selection of mostly remaining in sun-pointing mode with deployable panels incident to sun, opposite facing body mounted and deployable panels were paired.

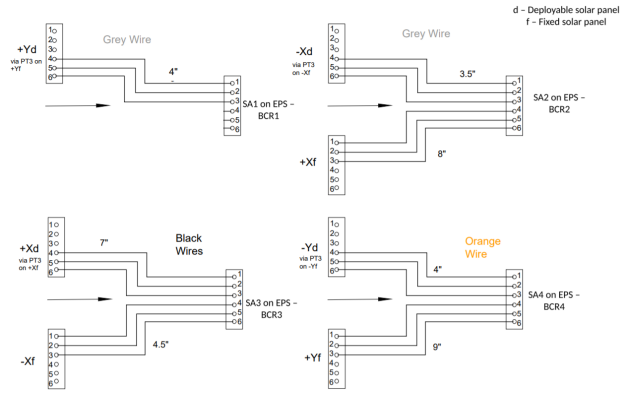


**Figure 3: Solar Panel Wiring Diagram**

## POWER BUDGET

In order to perform simulations on the total power usage and generation of the spacecraft, a power budget spreadsheet was created to keep track of how much power is used by each component in each of its power states, and which components are active in each of the various operational modes of the spacecraft. Together, this allowed the analysis team to easily determine the total amount of power used by the spacecraft (with overhead for voltage conversions) while being versatile enough to allow changing the parameters through the system design process with relative ease. Figure 4 below shows a sample subset of the power budget used in the DODONA analysis.

## INITIAL DE-SPIN

Upon reaching orbit, the first action of the CubeSat after deploying its stowed solar arrays will be to de-spin and dump excess angular momentum in order to stabilize its rotation and point the petal solar array at the Sun. To do this, magnetic torque rods are used, which interact with the Earth's magnetic field to impart a torque on the spacecraft, transferring the angular momentum of the spacecraft to the Earth. The control law that governs this action is called the B-dot control law. It depends on the measured body rates of the spacecraft and measured magnetic field of Earth. The controller then commands a magnetic moment that creates a torque in the opposite direction of the spacecraft's rotation effectively slowing its rotation. This action requires approximately 7.6 W of power to perform, and the amount of power generated and time required depends on the orientation of the spacecraft with respect to the Earth's magnetic field at the time of de-spin. This cannot be precisely predicted, as it depends on rotation rates of the launch vehicle itself, its interactions with the atmosphere during ascent, and errors in the thrust control during the ascent. For conservative estimates, an upper bound for the initial rotation

| | 1.Eclipse Cruise | | | | 2.BUS Tx | | | |
|---|---|---|---|---|---|---|---|---|
| main components powered on | power card, dual battery, Card A, B, C + No Tx | | | | UHF Transmitter | | | |
| POWER DRAIN | | | | | | | | |
| **BUS** | Duty Cycle | Option | Wattage | Power Drain | Duty Cycle | Option | Wattage | Power Drain |
| **ADACS** | | | | | | | | |
| ADACS | 100% | Typicall all motors running continuosly, 5 Hz telemetry | 5.60000 | 5.60000 | 100% | Typicall all motors running continuosly, 5 Hz telemetry | 5.60000 | 5.60000 |
| **CARD A** | | | | | | | | |
| Pic24 Flight Proc. (Lower PPM) | 100% | CPU active. Clock = 32MHz | 0.10000 | 0.10000 | 100% | CPU active. Clock = 32MHz | 0.10000 | 0.10000 |
| Gyros | 100% | Normal mode | 0.27000 | 0.27000 | 100% | Normal mode | 0.27000 | 0.27000 |
| Motherboard Module | 100% | Typical Operation | 0.00250 | 0.00250 | 100% | Typical Operation | 0.00250 | 0.00250 |
| **CARD B** | | | | | | | | |
| Battery Heater | 100% | Battery Heater | 0.40000 | 0.40000 | 0% | Battery Heater | 0.40000 | 0.00000 |
| Quiescent Power Draw | 100% | Quiescent Power Draw | 0.10000 | 0.10000 | 100% | Quiescent Power Draw | 0.10000 | 0.10000 |
| **CARD C** | | | | | | | | |
| EPS | 100% | Quiescent Power | 0.40000 | 0.40000 | 100% | Quiescent Power | 0.40000 | 0.40000 |
| **CARD D** | | | | | | | | |
| Stensat Beacon | 100% | Beacon Tx (Nominal Duty) | 1.68000 | 1.68000 | 0% | Beacon Tx (Nominal Duty) | 1.68000 | 0.00000 |
| **CARD E** | | | | | | | | |
| ADACS Interface Module | 100% | 12 volts | 0.00000 | 0.00000 | 100% | 12 volts | 0.00000 | 0.00000 |
| Magnetometer | 100% | In Use | 0.00150 | 0.00150 | 100% | In Use | 0.00150 | 0.00150 |
| **STRUCTURE** | | | | | | | | |
| Sun Sensor | 100% | active | 0.15000 | 0.15000 | 100% | active | 0.15000 | 0.15000 |
| **PAYLOAD** | | | | | | | | |
| **PEC** | | | | | | | | |
| GomSpace NanoCom AX100 (Rx) | 100% | RX (NanoCom) | 0.26400 | 0.26400 | 0% | RX (NanoCom) | 0.26400 | 0.00000 |
| GomSpace NanoCom AX100 (Tx) | 0% | TX (NanoCom) | 2.64000 | 0.00000 | 100% | TX (NanoCom) | 2.64000 | 2.64000 |
| Pic24 Fligth Proc. (Upper PPM) | 100% | CPU active. Clock = 32MHz | 0.10000 | 0.10000 | 100% | CPU active. Clock = 32MHz | 0.10000 | 0.10000 |
| Mux / RS232 circuits | 100% | idle | 0.00330 | 0.00330 | 100% | active | 0.02310 | 0.02310 |

| | | 5 volt power | 3.3 volt power | V Batt power | 5 volt power | 3.3 volt power | V Batt power |
|---|---|---|---|---|---|---|---|
| **EPS efficiency** | 0.90000 | | | | | | |
| **power consumption (W)** | | 0.62400 | 0.26730 | 8.34000 | 0.62400 | 2.66310 | 9.10000 |
| **Actual Power consumption (W)** | | 0.68640 | 0.29403 | 9.17400 | 0.68640 | 2.92941 | 10.01000 |
| **Boost Converter Efficiency** | 0.90000 | | | | | | |

**Figure 4: Sample Power Budget**

rate was set at about 10 degrees per second. To ensure that the combination of battery power and intermittent solar power during the spin will be sufficient to power the torque rods, simulations were run for 48 different starting orientations, spread evenly over $4\pi$ Steradians, and each orientation was computed for a Gaussian distribution of 75 initial spin rates imparted by the launch vehicle and deployment system, yielding 3,600 different simulation cases.

These simulations use a combination of data generated from an in-house 6 degrees of freedom simulator (6DOF) visualized through LabView and STK, combined together in Matlab to compute the power produced and used at each timestep. The simulations run through the 6DOF utilizing the spacecraft's flight controller using a B-dot detumbling control algorithm with the initial orientation and spin rate, the initial position and velocity in orbit, and the IGRF10 Geomagnetic Field Model with updated 2019 coefficients.[3] To determine the amount of time it will take to de-spin the spacecraft, the orientation of the spacecraft at each timestep during the de-spin process, and state of the system at every timestep was tracked.[4] A timestep of one second was used. After generating and saving this ephemeris and attitude data, it was fed via Matlab into an STK scenario containing a 3D model of the CubeSat with all of its solar panels, defined as STK-compatible solar panel objects with their respective efficiencies. The solar panel simulator tool was then used in STK to determine the amount of power generated at every timestep in the simulation. A 60 second timestep was used. The tool uses ray tracing techniques in order to determine which solar cells are lit by the Sun and how much power they produce at the given spacecraft position and orientation. This data was then combined in Matlab with data from the spacecraft's power budget, listing how much power is used in a given mode. Together, all this data was used to compute the state of charge of the batteries over the course of the de-spin for each of the 3,600 cases.

The plot in Figure 6 shows the maximum depth of discharge (DOD) of the battery for each of the attitude and spin cases considered. In order to be considered a successful de-spin maneuver, the battery should not be depleted, and for an optimal de-spin, the DOD should not exceed 30%.

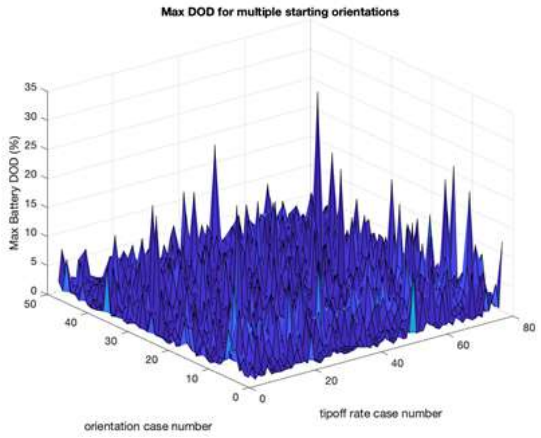


**Figure 6: Maximum Battery DOD for each case**

Analyzing the data used to form the plot, the maximum battery depth of discharge for any of the 3,600 cases is 31.5%, slightly above the optimal threshold of 30% but well below depleting the battery completely. For the most part, the runs yield DOD values of less than 10%. Aside from the few outliers, the fluctuations of DOD with re-

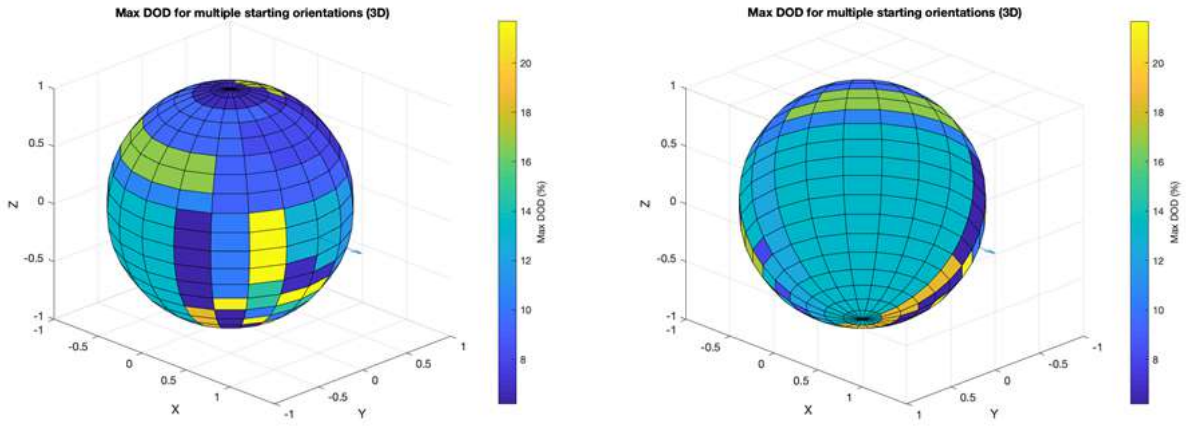


**(a)** front view **(b)** rear view

**Figure 5: Maximum Battery DOD for each attitude**

spect to the Gaussian distribution of input spin rates are evenly distributed, indicating that there is a low correlation between spin rate magnitude and battery DOD during de-spin.

Figure 5 above shows the maximum DOD for each of 48 starting orientations, wrapped as a colormap on a sphere. This color distribution allows us to see which initial attitudes are most beneficial and least beneficial for the de-spin process. Looking at the plots, initial orientations towards magnetic north are generally more favorable than those with initial orientations that line up the spacecraft's z-axis with the magnetic south pole of the Earth. The exact cause of this result is uncertain. An initial theory was that the body rate vector was aligned with the ambient magnetic field line causing initial lack of control authority which causes a higher de-tumbling duration and therefore higher DOD. This theory was ruled out as both North and South facing initial orientations should suffer from this and the initial rates are sufficiently randomized that the initial rotation and orientation should not be coupled in this way. Further analysis of the data shows that for the anomalous cases with high DOD, the 10,000 second GNC simulation runtime was not enough to de-spin the satellite, resulting in low power input and high power usage.

Moving forward, this data will be used to target more refined simulations in key areas of interest, and to cross reference with simulations from the launch provider to see what ranges of orientations are expected, and the probability of certain initial attitude configurations vs others. The estimated deployment orientation and rotation rates can then be propagated forward before activating the flight controller, mimicking on orbit behavior and providing even better controller performance estimates. This greatly reduces the number of possible initial rotations and orientations allowing a greater number simulations to be run with higher statistical fidelity.

## POWER SYSTEM MAINTENANCE

After determining through simulation that the power system will be sufficient to de-spin the spacecraft, initial maintenance and testing on the hardware began. The built-in under voltage protection system has a threshold value of 6.2 V, when the battery voltage drops below this value, the power system shuts down all output power lines until the battery is recharged to above 7 V. This complete reboot is not very consistent and often turns on all devices present on the CubeSat causing the battery to drain faster. A fix for this situation is discussed under brownout code implementation.

To always maintain the batteries at a nominal voltage of 7.4 V during ground testing and storage, a simple DAQ (data acquisition) system was employed to log and plot satellite voltage over set intervals of time. The DAQ system was built using open source python libraries to interface with laboratory measurement devices using the SCPI (Standard Commands for Programmable Instruments) syntax and commands. This system also proved to be useful in identifying anomalous behavior during ground testing as it directly corresponded with a voltage surge or dip. This surge was directly correlated to unknown beacons being transmitted at unscheduled times, which was ultimately identified as an issue with the flash memory chip. Closely tracking the power system and comparing it to the timestamp of the unknown beacons h0elped locate and eventually resolve an issue across other spacecraft subsystem.

Additionally, analysis was performed to estimate the depth of discharge of the battery system during stow for launch vehicle. For this purpose, manufacturer lot testing data was used to generate a surface fit model of basic battery specifications such as voltage, capacity, and discharge rate. This model was used as the basis to make predictions. Input for this mathematical model was calculated from the data collected by the DAQ system.

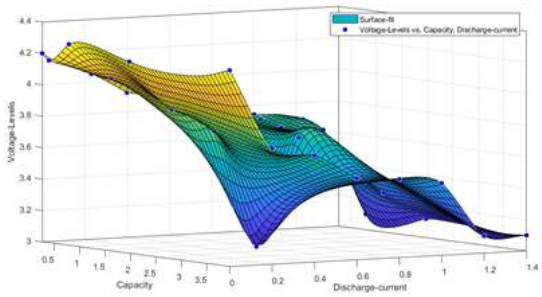


**Figure 7: Surface Fit Model**

## POWER SYSTEM TESTING

All components of the power system, namely the EPS board, battery system, and solar panels, were tested prior to integrating onto the satellite. This section will discuss the various tests that were performed and their results. The subsequent section will detail the issues encountered and how they were resolved.

### *EPS Qualification*

In addition to visual inspection, a series of tests were performed to validate EPS operations such as power conditioning, protection circuitry, BCR performance, and USB charging capabilities. The battery system was not used during this testing phase, instead, a power supply set to a nominal voltage and current limit with a series resistor was connected to simulate the battery.

Power Conditioning Test validated the performance of the 3.3 V and 5 V regulators present on the EPS board. To perform this test, the simulated battery was first con-

nected to the EPS system, then, the RBF switch and the separation switch were closed. A digital multimeter was used to read the regulated output from the PC-104 header on the EPS board.

To test the undervoltage protection circuitry present on the EPS module, the simulated battery voltage was gradually lowered below the threshold value of 6.2 V. At this point, all output power buses read zero indicating that they were shut down.

BCR performance was tested to validate maximum power point tracking behavior, to do this an oscilloscope was placed in between the solar array input and the EPS module. The output waveform observed validated MPPT and showed the panel voltage switch to open circuit values during tracking.

End of charge operation was demonstrated by gradually increasing the simulated battery's voltage above the threshold of 8.2 V and by placing an ammeter inline with the solar array input. As the voltage went above this threshold the input decreased to 0 A.

USB charging is not as effective as the input from the solar arrays, it should only be used as add on. To validate this capability, the satellite bus was turned on and connected to a local computer using a terminal interface. Command was then sent to query EPS telemetry, the telemetry was checked to verify that the battery was charging.

### *Battery System Testing*

This system was tested extensively as it often proved to be the point of failure in several ground operations tests. Each Li-polymer cell was visually inspected for any visible damage before they were integrated into the respective battery boards. Each board was visually inspected under a microscope, physical components such as fuses, and resistors were tested and finally, all surface traces were checked. After the cells were integrated into the boards, each board was tested as a standalone DC supply. This was done by simulating BCR input through a power supply and closing the RBF switch and separation switch. Connecting a digital multimeter to the positive battery bus pin on the PC-104 interface read the net voltage on the battery board.

Cells that failed during ground testing were retrieved and put through multiple charge-discharge cycles to test capacity retention. In most situations, it was identified that the cells failed because of a high discharge rate or sometimes because of over discharging the cells. Further testing and time revealed that the issue was in fact with the battery board and not with the cells. The following section discusses how it was identified and the solution sought.

To verify cell balancing on the boards, each battery was connected to a custom load board and allowed to discharge. All cells were monitored individually using exclusive voltmeters and ammeters.

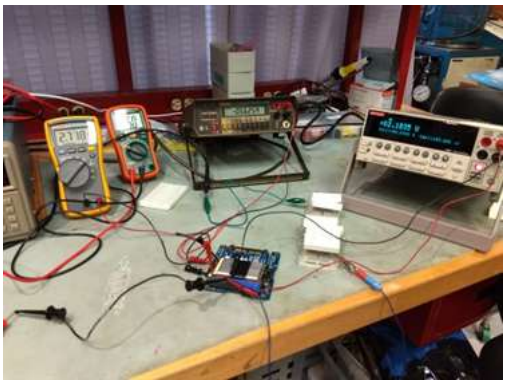

**Figure 8: Remote Battery Board under Test**

### *Solar Panel Qualification*

All seven solar panels were tested individually to verify operation. Panel I-V characteristics were used to determine open circuit values. Orbital solar flux environment was recreated using a halogen work lamp placed at a calculated distance from the solar panel. A custom load board was attached to the panels to maintain them at ideal operating conditions. Additionally, provisions were made to the load board to support testing of 2 cell panel. Figure 9 illustrates the layout.

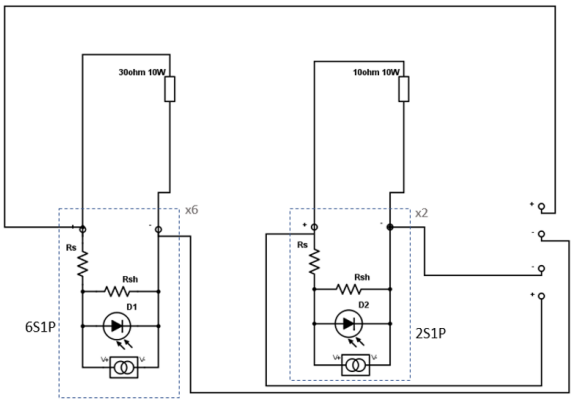


**Figure 9: Solar Panel test layout**

## ISSUES ENCOUNTERED

### *Severe Battery Drains*

The power system was often the point of failure during the initial phases of ground operations testing. This was mainly because the Li-polymer cells on the boards would buckle, causing the entire system to shut down. To debug this issue the same framework as mentioned in the battery system testing section was employed. First, the damaged cells were inspected and tested individually, then a com-

prehensive inspection of the board was carried out. During this period, a structured procedure was put together to enable quick swapping of new cells into the battery boards. This will be covered in detail under the integration section.

Once these tests were passed, new cells were integrated, and the boards were put through a charge-discharge cycle to verify cell balancing. It was in this test that it was identified that the battery board did not discharge in a uniform manner. It would only use certain cells on the board causing them to get overworked and eventually fail. Additionally, it was also discovered that the protection circuitry on the boards was faulty, this allowed exposure to overvoltage and overcharging.

The issue was resolved by replacing the 20 W h battery module with a spare. The spare was flight qualified using the same test framework.

### *EPS Current Leakage*

In the standard stow configuration, with the RBF switch closed and separation switch open (launch vehicle configuration), it was observed that there was a small current draw from the battery flowing back to the maximum power point tracker on the EPS. An average estimate for complete drain of the battery system due to this issue was obtained from the DAQ system, it was found to be 156 hours which is drastically low compared to an otherwise nominal value of approximately two months. However, a fix for this is provided by the manufacturer on request, it is a PCB which operates as a slave switch preventing back flow. The separation switch acts as the master here. This method allows system charging while on launch vehicle with the only downside that it brings down the end of charge voltage from 8.2 V to approximately 7.7 V. This circuit was attached to the motherboard and connected to respective switches and pins as per manufacturer guidelines. Refer to Figure 2 for the schematic on switch operation.

## BROWNOUT CODE IMPLEMENTATION

One of the potential failure modes identified by USC's 2nd satellite was inefficient battery management and excessive power consumption. Post mission forensics showed that the satellite entered an infinite reboot loop because the power up sequence was not regulated. Each time the processor turned on it immediately activated the magnetometer, transmitter, payload, gyroscopes, reaction wheels, sun sensor, and bus boards. Each subsystem alone did not require much power, however turning them all on at once required an amount of power greater than what could be supplied by the batteries at that time. The strain on the batteries was so great that the entire system would blackout and restart.

The proposed solution was to program a brownout power up contingency in the flight software. Software was added onboard as part of the scheduled tasks that run every second. These new pieces of code queried the voltages from the various lines on the EPS and the 10 most recent values were analyzed to produce a more accurate voltage reading, translated further into a low, medium, or high battery state. Depending on the battery state there was a specific action taken. Table 2 shows the action taken by the processor at each potential battery state and the amount of power needed in each state.

While power management is incredibly important to the success of a satellite it is by no means the only aspect of mission assurance that was considered. Contingency plans were discussed to mitigate the effects of losing communication with the sun sensor. If the sun vector is lost, then the attitude, determination, and control system will not have the necessary information to point the satellite at the sun, which will inevitably result in power issues. One potential solution to this issue is to measure the voltage on each of the 4 body mounted solar panels

**Table 2: Processor Action corresponding to Battery State**

| State | Action | Power Used in Each State |
|---|---|---|
| Tipoff Powerup | Payloads remain off until sun pointing is achieved | 13.5602 Watts |
| Low (6.6V – 7V) | Cut power to payload | 13.5602 Watts |
| Medium (7V – 7.4V) | Do nothing, record value and transmit over beacon | 20.5602 Watts |
| High (7.4V – 8.4V) | Do nothing | 20.5602 Watts |
| Reboot After Blackout | After reboot, only turn on transmitter, record blackout event and transmit over beacon | 9.5602 Watts |

and one of the deployed solar panels to generate a sun vector based on those values. Methods for tracking the sun in space can be taken from solar farming techniques on earth. The equations can be easily implemented as there is a wealth of literature on the subject in the paper by Mousazadeh.[5]

## INTEGRATION AND TEST PROCESS

Given the need to first resolve the power system's functionality for ground operations and a rapid development timeline for the mission, a piecewise qualification approach was utilized with focus on standardizing test set ups and integration procedures. This minimized risk to ground and flight hardware, while maximizing likelihood of identifying underlying abnormal behavior, rather than minor inconsistencies. The general integration and test process required one team member executing the set up, test or integration, and verification, while a peer director oversaw the activity, carefully tracking activity per a predefined procedure and noting any risks or necessary deviations.

Battery replacement became a commonly executed activity while other components of the power system were troubleshooted. To expedite this activity, off the shelf batteries were selected with matching cell properties to their space-grade counterparts.They required minor modification to integrate directly to the battery boards but sufficed for terrestrial testing with a high degree of success. The structured procedure for cell replacement included:

- de-integration of battery boards from the satellite bus development stack
- de-soldering of individual battery cells
- preparation of individual cells
- re-soldering of new cells onto battery boards
- standalone testing of boards with replaced cells.

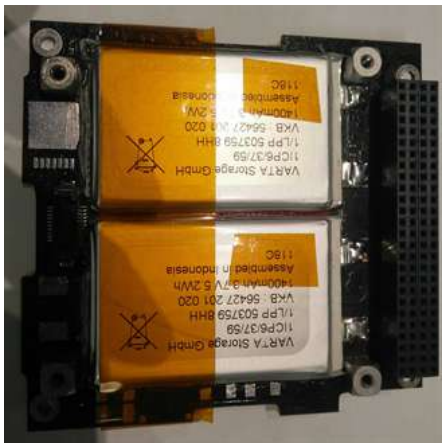

**Figure 10: Lower Level DBB fit with new cells**

Since these batteries were intended for terrestrial testing only, they were secured with Kapton tape as a mechanical force supplement to the soldered pads, rather than secured with specialty potting material, as necessary for final integration for delivery to space. Additionally, these testing batteries were assigned unique labels and voltage and exact battery board location (of the six possible locations) was tracked in detail through every step of the procedure. This ultimately enabled diagnostic of the origin of the power system failure.

**Figure 11: Remote Battery board ready for integration**

Individual and integrated components were first verified on the development stack, which was more rapidly integrated and de-integrated. The flight configuration, with the nanosat small form factor size, was much more time intensive to assemble. It also presented specific risks relative to shorting the batteries and possibly damaging the power system. To minimize these risks, the team again made use of structured procedures with careful peer oversight. Additionally, the most sensitive integration steps were identified, to enable additional personnel to assist with these steps and where possible, mechanical changes were employed. Battery board posts that were previously live with stainless steel hardware directly connected to battery test points were replaced with nylon hardware. Where boards were still under development and therefore not yet conformally coated for flight had exposed circuit traces, Kapton tape was utilized to prevent accidental shorting. During integration, the outer structural metal chassis was covered with anti-static bags, so that rows of pins that included live battery voltages and grounds could not accidentally short on these surfaces.

Another strategy for rapidly enabling testing was building custom wiring harnesses in house. These included harnesses for connecting directly to the individual solar panels and to the electrical power system through the battery charge regulators. This was both for functional component testing, debugging, and ultimately for the flight

harnesses for the spacecraft. For testing, the harnesses were constructed to directly interface with a breadboard with specific test points to monitor voltage and current under a variety of conditions. For functionality, it enabled us to precisely charge and vary conditions through a solar panel simulator power supply. This in turn allowed us to validate the software checking power levels relative to operation mode, including validating initial orbit operations. For flight, this enabled a custom configuration of the solar panel wiring to maximize power generation during sun pointing mode.

Finally, following resolution of independent power system issues, the power system was finally validated alongside the entire integrated spacecraft during our 8 hour burn-in. This allowed us to check all flight hardware over a long run time, as if the satellite was operating in orbit, beginning with tip-off following launch through nominal orbit operations. All hardware, including the power system, successfully demonstrated the appropriate boot up and initialization sequences, then moving into regularly scheduled satellite activity.

**Figure 12: Major satellite bus components prepared before integration**

## CONCLUDING REMARKS

Through this project the Space Engineering Research Center has further established its technical approach in space system integration and test. Given the accelerated DODONA mission timeline, development was necessarily rapid in nature. Evaluation of hardware/software systems individually and then in an integrated environment was scheduled thoroughly and methodized to allow execution within the set deadlines. Parallel testing of different systems was often the choice unless the component required motherboard time, hindering software tests. Known risks during the course were met with a considerable amount of precaution.

Documentation was given a lot of importance, all processes and modifications to hardware/software were recorded and a simple version control software was used to keep track of all changes. This proved to be very useful in troubleshooting. Further, all documents will be archived with the intention of providing guidance for a future mission with similar requirements and expectations.

## ACKNOWLEDGMENTS

We thank Professor David Barnhart for creating the opportunity to design and build this CubeSat, and his guidance through the course of the project. The authors acknowledge with gratitude, the help and support from fellow members at the Space Engineering Research Center, USC. We also wish to thank Clyde Space Ltd. and Pumpkin Space Systems for their resources. The team cites the following software suites for providing the environment to perform simulation and analysis, LabVIEW from National Instruments, Systems Tool Kit (STK) from Analytical Graphics, Inc and MATLAB from MathWorks. Finally, we would like to recognize Vector Launch Inc for choosing to partner with us and making this endeavour successful.

## REFERENCES

1. Craig S Clark. A universal power system architecture: One topology for earth and planetary orbits. In *Space Power*, volume 502, page 135, 2002.

2. Craig Clark and Evelyne Simon. Evaluation of Lithium Polymer technology for small satellite applications. 2007.

3. Arnaud Chulliat, William Brown, Patrick Alken, Susan Macmillan, Manoj Nair, Ciaran Beggan, Adam Woods, Brian Hamilton, Brian Meyer, and Robert Redmon. Out-of-Cycle Update of the US/UK World Magnetic Model for 2015-2020. 2019.

4. Michael Aherne, Tim Barrett, Lucy Hoag, Eric Teegarden, and Rohan Ramadas. Aeneas–Colony I meets three-axis pointing. 2011.

5. Hossein Mousazadeh, Alireza Keyhani, Arzhang Javadi, Hossein Mobli, Karen Abrinia, and Ahmad Sharifi. A review of principle and sun-tracking methods for maximizing solar systems output. *Renewable and sustainable energy reviews*, 13(8):1800–1818, 2009.